2015 IEEE International Conference on Advanced Intelligent Mechatronics (AIM)
July 7-11, 2015. Busan, Korea

Autonomous Formation Selection For Ground Moving Multi-Robot Systems

Shuang Yu[1] and Jan Carlo Barca[2]

Abstract— **Multi-robot systems have many useful real world applications including disaster management, exploration and surveying. Formation control is critical in these contexts as the success of groups often depend on the ability to generate and maintain particular formation shapes. It is also important that a multi-robot system can evaluate and select appropriate alternative formations when an ideal formation cannot be upheld, particularly in dynamic real world scenarios. A distributed formation selection mechanism that addresses these issues by enabling groups of unmanned ground vehicles to autonomously select, scale and morph formation shapes when navigating through dynamic environments is presented in this paper. Experiments on non-holonomic ground moving robots demonstrate the suitability of the proposed technology.**

I. INTRODUCTION

The research community has recently shown a growing interest in multi-robot systems (MRS) due to their high-impact application areas, including disaster management, environmental monitoring, exploration and surveying. The advancement of this technology has created a demand for distributed mechanisms that can monitor and regulate formation configurations, as the success of groups often depends on the ability to preserve appropriate geometric structures [1]. As a result, formation control mechanisms that enable MRS to generate and preserve formations have been widely studied [2], [3], [4], [5], [6]. However their ability to select, scale and morph formations autonomously in dynamic environments has received much less attention. It is therefore important to address this issue as most real world situations require continuous adaptation to unpredictable environments, and because it is desirable to minimize the load on human operators in MRS contexts [7].

Some efforts in addressing this problem have therefore been made. Relevant works include the: i) graph theory based techniques presented in [8], [9], which offer a theoretical framework for how formations can be scaled up and down, ii) method described in [10] which enable swarms of simulated robots to identify appropriate formation scales on the basis of the number of robots in the system, and iii) research presented in [11] that demonstrates how groups of non-holonomic ground moving robots can scale and morph formations autonomously. A drawback with the work presented in [8], [9], [10] is that only varying formation sizes are considered. This is not ideal as teams of robots are sometimes required to alter their formation shapes to accomplish a task (e.g. if the robots have formed a broad formation and must navigate through a narrow opening). The main drawback with the work presented in [11] is that the authors did not demonstrate that their robots can select alternative formation scales and shapes in a distributed manner.

Researchers have also sought inspiration from biological morphogenesis in their efforts to address the above problem. In [12] the authors present a morphogenesis inspired neighborhood adaption mechanism that enables groups of e-puck robots to distribute across a pre-defined target pattern according to the number of robots in the system. However, they do not scale the actual pattern up or down when the number of robots do not fit the original pattern. This makes it difficult to maintain appropriate formations when the number of robots changes dramatically. The problem of selecting appropriate formation shapes is furthermore not addressed. In [13] a morphogenesis inspired adaptive pattern formation mechanism for e-pucks is presented. A drawback with this technique is that the generated formations are based purely on circular patterns. This is a problem as different tasks often require radically different target patterns. A more flexible technique that can respond effectively to a broad range of different scenarios is therefore required.

We address the above drawbacks by proposing a distributed technique that enable MRS to select, scale and morph formation shapes when navigating through dynamic environments. The proposed technology builds on the work presented in [11] and is validated on real non-holonomic ground moving robots.

The remaining parts of this paper are structured as follows; Section 2 offers an overview of the system design, along with detailed descriptions of the proposed formation control mechanisms. Section 3 describes results from experiments that have been designed to evaluate the proposed technology. Finally, conclusions and suggestions for future research are presented in Section 4.

II. AUTONOMOUS FORMATION SELECTION

In this research, we assume that the robots have been assigned from the outset an *ideal formation* for the task at hand and a series of *alternative formations* with various scales. Any two dimensional formation can be assigned to the robots as long as the robots are connected. We also assume that the robots are sometimes required to alter the ideal formation to successfully navigate through dynamic environments without experiencing collisions. Different formations have different characteristics that make them ideal for particular tasks, for

[1]Shuang Yu is with Department of Electrical and Computer Systems Engineering, Monash University, Melbourne, Australia shuang.yu@monash.edu

[2]Jan Carlo Barca is with Clayton School of Information Technology, Monash University, Melbourne, Australia jan.barca@monash.edu

example, a maximum coverage formation covers an area with the minimum number of robots, while a linear formation makes it possible to move through narrow openings. The *ideal formation* should therefore be selected according to the task and hand. Additionally, the MRS should always seek to preserve the ideal formation.

To achieve this aim, the proposed technique iterates through a four stage process that involves: 1) sensing and pre-processing, 2) local decision making, 3) distributed agreement and 4) navigation. In Stage 1, each robot collects information from its immediate surroundings by means of an on-board distance measurement sensor, and prepares this information for further processing. In Stage 2, the collected data is fed into a decision tree that enables each robot to identify a *locally preferred formation*. These locally preferred formations are then shared with neighbouring robots so that consensus can be reached on a group level in Stage 3. Each robot calculates its desired position in the new formation and navigates towards the target location in Stage 4, if a formation change is required.

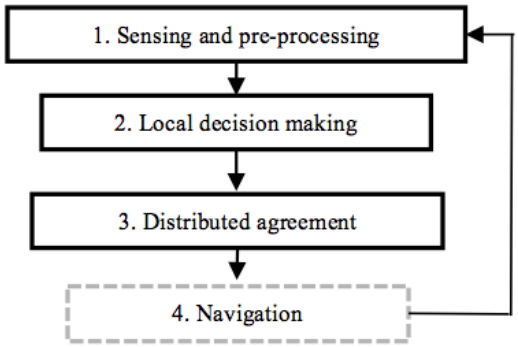

Fig. 1: System overview

An overview of the proposed technique is given in Fig. 1. Detailed descriptions of Stages 1 through 3 are provided in the following subsections. The reader is referred to [11] for a detailed description of Stage 4.

A. Sensing and Pre-Processing

In Stage 1 distances to obstacles that appear within sensing radius r_s of robot R_0 are collected by means of an on-board distance measurement device with swipe angle S_{angle}. If an obstacle is detected within this region, it is regarded as blocking the path of R_0, and further information about the surrounding obstacles and robots is obtained.

To collect information about the surrounding obstacles and robots, we first define the forward direction for R_0 as the y-axis of the robot's orientation, and the x-axis as being perpendicular to the forward direction, as illustrated in Fig. 2. With N obstacles and M robots within the sensing region of R_0 we also define relative angles $\theta_{obs,i}$ to the surrounding obstacles, and $\theta_{r,i}$ to the surrounding robots. The Euclidean distance $d_{obs,i}$ to each obstacle and $d_{r,i}$ to each surrounding robot is then projected onto the x-axis of R_0 according to

$$d'_{obs,i} = d_{obs,i}\sin(\theta_{obs,i}) \tag{1}$$

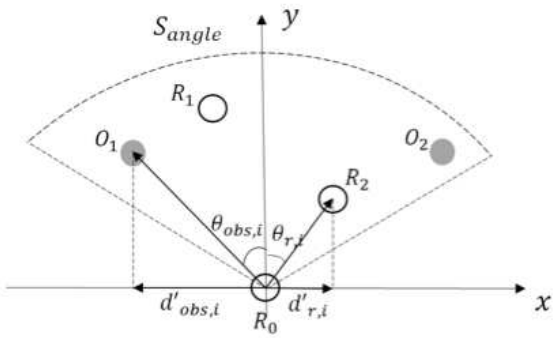

Fig. 2: Calculating the projected distance between the closest obstacle and the closest robot

$$d'_{r,i} = d_{r,i}\sin(\theta_{r,i}) \tag{2}$$

to determine if there is sufficient empty space ahead of the robot to allow R_0 to move forward. We furthermore arrange these projected distances with $d'_{obs,1} < d'_{obs,2} \ldots d'_{obs,j} < 0 \leq d'_{obs,j+1} \ldots < d'_{obs,N}$ and $d'_{r,1} < d'_{r,2} \ldots d'_{r,j} < 0 \leq d'_{r,j+1} \ldots < d'_{r,M}$.

With $d'_{r,min}$ being the x-coordinate of the robot who has the shortest projected distance on the x-axis to robot R_0 we calculate $d'_{obs,min}$ according to

$$d'_{obs,min} = \begin{cases} d'_{obs,j+1} & if\, d'_{r,min} < 0 \\ \min(|d'_{obs,j}|, |d'_{obs,j+1}|) & if\, d'_{r,min} = 0 \\ d'_{obs,j} & if\, d'_{r,min} > 0 \end{cases} \tag{3}$$

B. Local Decision Making

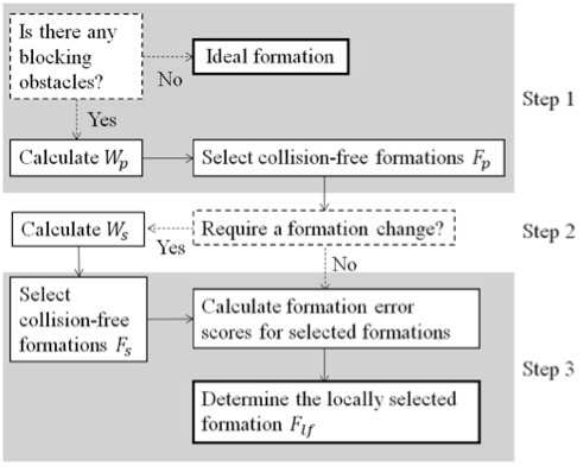

Fig. 3: Overview of Local Decision Making Process

Stage 2 enables each robot to determine if a formation change is required and to select its own *locally selected formation* out of the collision-free formations. An overview of the process is provided in Fig. 3.

At this stage, the first step is to examine the sensor data from the last stage as indicated in Fig. 3, Step 1. If no obstacle has been detected, the robot will prefer to maintain

the ideal formation and no further processing is required. In cases where one or more obstacles have been sensed, a formation change may be required to avoid collisions. Alternative formations will be evaluated according to the following criteria:

1) The robot's target destination should be reached without collisions

2) The new formation should introduce the shortest possible travelling distance

3) Unnecessary transitions between alternative formations should be avoided

Alternative formations that only differ from the ideal formation in scale are given higher priority to be evaluated in order to increase the likelihood of preserving the ideal formation shape. Alternative formation are represented by $F_{m,n}$. They are classified by the formation type, or intuitively, the formation shape, m and its associated formation scale n. Scaled versions of a formation type is achieved by changing the inter-robot distance $D_{m,n}$. Alternative formations $F_{m,n}$ are evaluated in three steps as described in Fig. 3, the intermediate output formations from the three steps are represented by F_p, F_s and the final output of this stage, the locally selected formation, is F_{lf}.

In Step 1, the parameter W_p is calculated for each robot as described in

$$W_p = \begin{cases} |d'_{obs,min}| + |d'_{r,min}| & if N \neq 0 \\ r_s + |d'_{r,min}| & if N = 0 \end{cases} \quad (4)$$

This parameter measures the projected distance between the closest obstacle and the closest robot to the forward direction vector. As indicated in Step 1, W_p is used to determine if an alternative formation is collision-free, considering all the surrounding obstacles and robots. The condition for an alternative formation $F_{m,n}$ to be selected in this step as one of F_p is

$$F_{m,n} \in F_p, \ if D_{m,n} \leq W_p - t_s \quad (5)$$

where

t_s: Safety distance

Safety distance t_s represents the space to be left between the robots and obstacles and is introduced to ensure that the locally selected formation satisfies Criterion 1.

Step 2 checks if all the formations in F_p require a change in shape. If no alternative formations which require only a change in scale from the ideal formation can be formed without collisions, a change in formation type is required. In this case, the neighbouring robots change their relative positions, therefore they should not be used as references for the clear path width. Hence the parameter W_s is calculated as in

$$W_s = d'_{obs,j+1} - d'_{obs,j} \quad (6)$$

W_s measures the projected distances between the two obstacles that are closest to the forward direction vector, as indicated in Fig. 4.

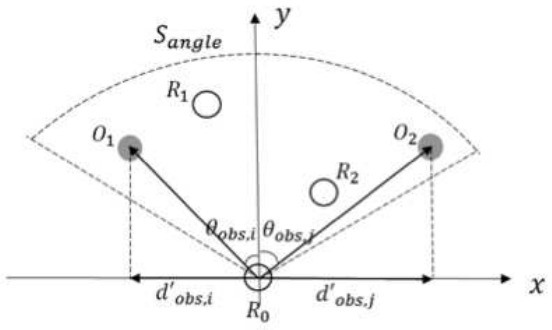

Fig. 4: Calculating the projected distance between the closest obstacles

Then in Step 3, another group of collision free formations F_s is selected from

$$F_{m,n} \in F_s, \ if D_{m,n} \leq W_s - t_s \quad (7)$$

In Step 3, alternative formations are evaluated. If a change in formation type is required, formations in F_p are evaluated, if no change in formation type is required, formations in F_s are evaluated. In order to satisfy Criterion 2 and Criterion 3, F_s or F_p are evaluated according to

$$E_i = C_i e_i \quad (8)$$

where

E_i : Formation error score

C_i : Formation state factor

e_i : Euclidean distance between current and target positions

The formation with the smallest E_i value is selected by the robot to be the locally selected formation F_{lf}. Formation state factor C_i is introduced to avoid unnecessary transitions, as empirical results show that robots have a tendency to select the more compact formations when only e_i is taken into account, even if a more compact formation is required, which in turn results in an unstable and highly fluctuant system. The value for C_i is chosen such that E_i for the more compact formations is amplified, and they are less likely to be chosen as F_{lf}. Also, the value of C_i for the ideal formation should be lower than that of the alternative formations in order to amplify its chance of selection.

C. Distributed Agreement

Once individual robots have identified locally selected formations, the group as a whole must reach a collective agreement on which formation to select. At this stage, F_{lf} is assigned to the robot as its initial formation state. Given the notation $\xi_i[k]$ for formation states of robot i during the collective stage, $\xi_i[0] = F_{lf}$. It is proven in [18] that distributed linear iterations offer fast convergence. Consensus is achieved by means of the weighted consensus mechanism in (9).

$$\xi_i[k+1] = W_{ii}\xi_i[k] + \sum_{j \in M} W_{ij}\xi_j[k], j = 1, ...M_i \quad (9)$$

with

$$W_{ij} = \frac{s_j k_j}{k_1 + k_2 + ... + k_{M_i}} \quad (10)$$

$$s_j = s_0 \frac{V_0}{V_j} \quad (11)$$

where

k : number of iterations

$\xi_i[k]$: current formation state of robot i

$\xi_i[k+1]$: next formation state of robot i

W_{ij} : weight on ξ_i at robot i

M_i : number of robots within robot i's communication radius

s_0 : step constant

s_j : step time of robot j

V_j : relative robot speed of closest obstacle to robot j

V_0 : standard robot speed

k_j : obstacle weight robot j introduced to its surrounding robots

The mechanism is designed such that the closer a robot is to obstacles, the higher its weight will become in the consensus process. Having a weight that is associated with the distance to obstacles exerts a bias on the robots that have more precise information about the surrounding obstacles. The robot that is closest to obstacles is also assumed to have the highest chance of crashing unless the formation is altered and the needs of this robot must therefore be attended to first.

Consensus is reached locally when the state differences of a robot i and its neighbours are smaller than a threshold T_s. Increasing this threshold will reduce the time it takes to reach consensus. However, if the threshold is too large, the discrepancy in the states will increase. It is therefore important to select a threshold that balances speed and accuracy. We have determined empirically that the state difference threshold should be less than 10% of the minimum state separation. This recommended threshold is used in Section 3.

Parameter s_j is the time interval between two consensus processes, which increases when the speed of robots is reduced with respect to obstacles, and it is therefore less urgent to change formations. Standard relative speed V_0 is determined according to the recommended speed of specific robots. The benefit of decreasing s_j is that consensus can be calculated at a slower pace to reduce energy consumption. It should be noted that there are lower and upper bounds for s_j. The value should always be larger than the communication round-trip delay to avoid using outdated data. The upper bound can be found empirically by identifying the time that enables the robots to reach consensus when the relative speeds of the robots are close to zero. This upper bound can be further increased if energy preservation is a major concern, however a higher risk of colliding with obstacles necessitates lower upper bounds. The k_j parameter is used to calculate weight W_{ij} and accounts for the distance between obstacles and the robots. This parameter is calculated according to

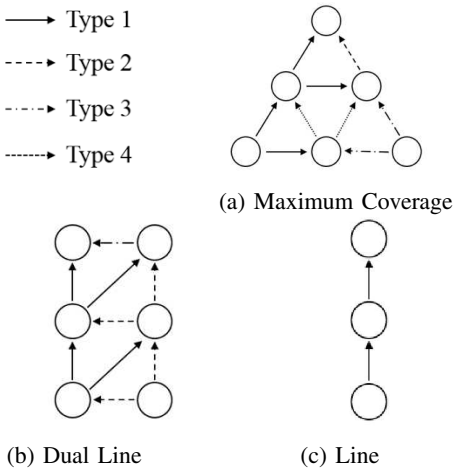

(a) Maximum Coverage

(b) Dual Line (c) Line

Fig. 5: Alternative formation types

$$k_j = exp(\frac{\frac{r_s}{d_{min}} - 1}{\tau}) \quad (12)$$

where

d_{min} : distance to closest obstacle, and $0 < d_{min} < r_s$

τ : time constant

III. EXPERIMENT DESIGN AND RESULTS

In this section, we validate the proposed formation selection mechanism by means of two experiments: one tests the convergence speed of the proposed consensus algorithm as the relative speed to obstacles increase, while the other evaluates the spatial adaptability to varying path widths. Each experiment was carried out 5 times and the mean of the results were calculated and presented in graphs of this section.

According to [14], [15], [16], several patterns can be used as maximum coverage formations. The optimal pattern depends on the communication and sensing ranges of the robots. Considering the constraints given by our technology and the connectivity requirements in this research, a triangular pattern was selected. The alternative formations used in our experiments are shown in Fig. 5. Different types of arrows between nodes represent different constraint types and each node represent one robot. Correspondingly, Tables II, III and IV display the distance and angle constraints used in each formation. These constraints have been adopted from [6].

In the experiments, two continuous rows of virtual obstacles are driven towards the MRS in order to simulate a narrow tunnel that the robots have to pass through. The formation states held by the robots at every time step are

TABLE I: Parameters for Implementation Specific Variables

Parameters	Value
S_{angle}	180°
t_s	436 mm
V_0	61.2 mm/s
T_s	0.1
s_0	1
r_s	570 mm
τ	0.4

TABLE II: Constraints for Maximum Coverage Formation

Types	Distance 1	Angle 1	Distance 2	Angle 2
1	r_s	30°	r_s	90°
2	r_s	−30°	–	–
3	r_s	−30°	r_s	−90°
4	r_s	30°	r_s	−30°

recorded throughout this process. Fig. 6 shows a scenario in which the MRS selected a Dual Line Formation to allow the robots to pass through the tunnel as the Maximum Coverage Formation, which is used as the ideal formation in our experiments, cannot fit through the narrow path. Since no formation selection algorithms that include obstacle avoidance have been proposed in existing literature, a comparison with other algorithms was not possible.

The MRS consists of five non-holonomic ground moving "eBug" robots [17], while an overhead camera connected to a computer acts as a pseudo-GPS which is used to emulate laser range finders with a 360° field of view. The computer also generates and moves the virtual obstacles that form the narrow corridor, while ZigBee networks enable the robots to communicate with the computer and neighbouring robots. Implementation specific parameters used by the formation selection algorithm are listed in Table I.

A. Robustness to Increasing Formation Speed

This experiment evaluated the algorithm's ability to converge to a formation while the relative speed of the robots, with respect to surrounding obstacles, was increased. The

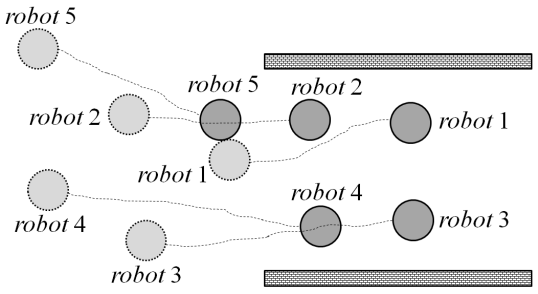

Fig. 6: The path ahead narrows, requiring a change from Maximum Coverage Formation. The MRS determines it is wide enough to accommodate Dual Line Formation, which reduces the total travelling distance comparing to Line Formation.

TABLE III: Constraints for Dual Line Formation

Types	Distance 1	Angle 1	Distance 2	Angle 2
1	$\frac{r_s}{\sqrt{2}}$	0°	r_s	45°
2	$\frac{r_s}{\sqrt{2}}$	0°	$\frac{r_s}{\sqrt{2}}$	−90°
3	$\frac{r_s}{\sqrt{2}}$	0°	–	–

TABLE IV: Constraints for Line Formation

Types	Distance 1	Angle 1	Distance 2	Angle 2
1	$\frac{r_s}{\sqrt{2}}$	0°	–	–

collision free path formed by the approaching obstacles was 783.5 mm wide. Starting from a relative speed of 22.8 mm/s, samples were taken in increments of 11.4 mm/s ending at 228 mm/s. The results from the experiment are plotted in Fig. 7.

The bottom solid line represents the time taken from when the obstacles are spotted to when the group agrees on a formation, while the dashed line represents the time taken before the robots have moved to their target position in the new formation. One can observe that the algorithm enables the robots to successfully converge to alternative formations, and thereby avoid obstacles, until the break point at 228.0 mm/s. The relative speed at the breakpoint equals 1.86 times the maximum speed of the robots.

B. Robustness to Narrow Paths

In this experiment, the stability over various path widths was tested. The separation that allows the formation to pass through the obstacle course was gradually reduced from 661.2 mm to 233.7 mm, plus a safety distance of 436 mm. Fig. 8 shows the average time taken to reach all intermediate formation types before the final formation was reached.

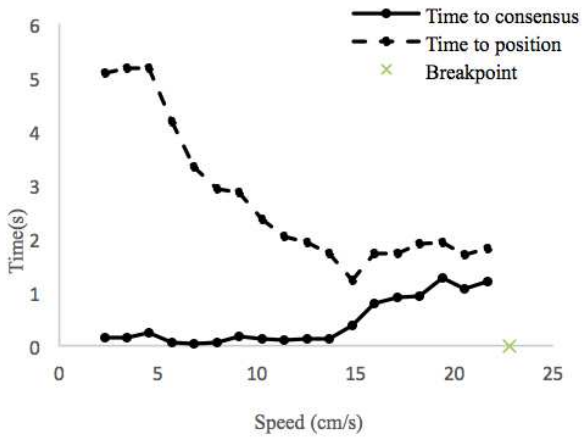

Fig. 7: Time vs. relative speed

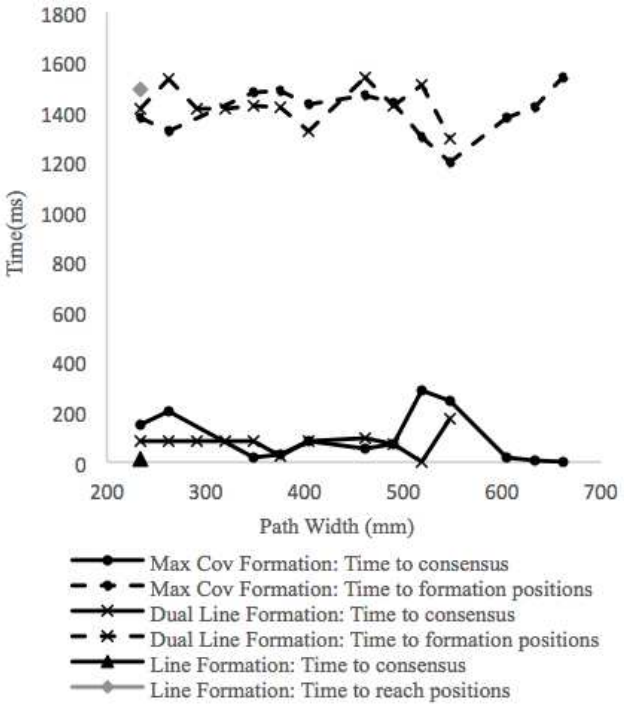

Fig. 8: Time vs. path width

One can observe that the MRS selects its formation according to the path width. The algorithm abandons the maximum coverage formation when the path width is narrower than 400 mm and thus enables the robots to pass through the obstacle course without experiencing collisions. The line formation is only formed when the path width is 233.7 mm, which demonstrates that the MRS will not converge to a more compact state than is necessary, in order to conserve energy. It should also be noted that the dual line formation is not formed when the path is wider than 547 mm, which justifies the use of formation state factor C_i.

IV. CONCLUSIONS

A distributed formation selection algorithm that enables non-holonomic ground moving robots to autonomously select and generate formations was presented in this paper. Experiments conducted on the proposed technology demonstrate that the algorithm enables the robots to navigate through environments with dynamic obstacles without experiencing collisions when the relative speed of the robots with respect to the obstacles is increased to 1.86 times the maximum speed of the robots. The experiments furthermore reveal that the formation selection mechanism is capable of selecting formations without introducing excessive travel distances. Future research can seek modifications in the consensus process to decrease the inaccuracy created by sensor noise in order to increase the system robustness.

ACKNOWLEDGMENT

S. Yu thanks Daniel Waghorn for his insight and assistance in refining and polishing this paper.

REFERENCES

[1] Barca, JC. and A. Sekercioglu. Swarm Robotics Reviewed. Robotica, Available on CJO 2012 doi:10.1017/S026357471200032X, pp. 1-32, 2012.

[2] B. Fidan, C. Yu and B. Anderson, Acquiring andmaintaining persistence of autonomous multi-vehicle formations,IET Control Theory Appl. 1(2), pp. 452-460, 2007.

[3] Z. Xue and J. Zeng, Formation Control Numerical Simulations of Geometric Patterns for Unmanned Autonomous Vehicles with Swarm Dynamical Methodologies, Proceedings of the International Conference on Measuring Technology and Mechatronics Automation, Zhangjiajie, China 2009.

[4] M. Mamei, M. Vasari and F. Zambonelli, Experiments of morphogenesis in swarms of simple mobile robots, Appl. Artif. Intell. 218(9-10), pp. 903-919, 2004.

[5] L. Barnes, M. Fields and K. Valavanis, Swarm formation control utilizing elliptical surfaces and limiting functions, IEEE Trans. Syst. Man Cybern. 39(6), pp. 1434-1445, 2009.

[6] Barca, JC., A. Sekercioglu, and A. Ford. Controlling Formations of Robots with Graph Theory. In: S. Lee, Cho, H., Yoon, K. and Lee, J. (eds) Intelligent Autonomous Systems 12. Springer Verlag, pp. 563-574, 2013.

[7] G. Podevijn, R. O'Grady, and M. Dorigo. Self-organised Feedback in Human Swarm Interaction, IRIDIA - Technical Report Series, Technical Report No.:TR/IRIDIA/2012-016, pp. 1-6, 2012.

[8] M. Mesbahi and M. Egerstedt (eds.), Graph Theoretic Methods in Multiagent Networks. Applied Mathematics (Princeton University Press, NJ, 2010) pp. 401.

[9] M.A. Haque and M. Egerstedt, Decentralized Formation Selection Mechanisms Inspired by Foraging Bottlenose Dolphins, Mathematical Theory Of Networks and Systems, 2008.

[10] Rubenstein, M.; Wei-Min Shen, Automatic scalable size selection for the shape of a distributed robotic collective, Intelligent Robots and Systems (IROS), 2010 IEEE/RSJ International Conference on , vol., no., pp.508,513, 18-22 Oct. 2010 doi: 10.1109/IROS.2010.5650906.

[11] Seng, L., Barca, J C. and Sekercioglu, A. (2013) Distributed Formation Control in Cluttered Environments. Presented at: 2013 IEEE/ASME International Conference on Advanced Intelligent Mechatronics (AIM).

[12] Meng, Y., Guo, H. and Jin, Y. A morphogenetic approach to flexible and robust shape formation for swarm robotic systems, Robotics and Autonomous Systems. vol 61, pp 25-38, 2013.

[13] Jin, Y., Guo, H. and Meng, Y. A Hierarchical Gene Regulatory Network for Adaptive Multirobot Pattern Formation, IEEE Transactions on Systems, Man and Cybernetics, vol.42, no.3, pp 805-816, 2012.

[14] L Xiao-Yuan LS-B, G Xin-Ping, Automatic generation of min-weighted persistent formations, Chinese Physics, pp. B 18(8):3104-3114, 2009.

[15] Xiaole Bai, Santosh Kumar, Dong Xuan, Ziqiu Yun, Ten H. Lai, Deploying Wireless Sensors to Achieve Both Coverage an Connectivity, MobiHoc, pp. 131-142, 2006.

[16] Ming Ma, Yuanyuan Yang, Adaptive Triangular Deployment Algorithm for unattended Mobile Sensor Networks, IEEE Transactions on Computers, pp. 946-958, 2007.

[17] DAdemo, N., Lui, W. L. D., Li, W. H., Sekercioglu, Y. A., Drummond, T. eBug-An open robotics platform for teaching and research. Proc. ACRA, 2011.

[18] Lin Xiao, Stephen Boyd, Fast Linear Iterations For Distributed Averaging, Conference on Decision and Control, pp.901-906, 2003